



Compact and flexible harmonic generator and three-color synthesizer for femtosecond coherent control and time-resolved studies

C. BURGER,^{1,2} W. F. FRISCH,² T. M. KARDAŚ,³ M. TRUBETSKOV,¹
V. PERVAK,^{1,4} R. MOSHAMMER,⁵ B. BERGUES,^{1,2} M. F. KLING,^{1,2}
AND P. WNUK^{1,2,3,*}

¹Max Planck Institute of Quantum Optics, D-85748 Garching, Germany

²Department of Physics, Ludwig-Maximilians-Universität Munich, D-85748 Garching, Germany

³Institute of Experimental Physics, Faculty of Physics, University of Warsaw, 02-093 Warsaw, Poland

⁴Ultrafast Innovations GmbH, D-85748 Garching, Germany

⁵Max Planck Institute of Nuclear Physics, D-69117 Heidelberg, Germany

*pawel.wnuk@mpq.mpg.de

Abstract: Intense, multi-color laser fields permit the control of the ionization of atoms and the steering of electron dynamics. Here, we present the efficient collinear creation of the second and third harmonic of a 790 nm femtosecond laser followed by a versatile field synthesizer for the three color fields' composition. Using the device, we investigate the strong-field ionization of neon by fields composed of the fundamental, and the second or third harmonic. The three-color device offers sufficient flexibility for the coherent control of strong-field processes and for time-resolved pump-probe studies.

© 2017 Optical Society of America

OCIS codes: (020.2649) Strong field laser physics; (230.4320) Nonlinear optical devices; (320.5540) Pulse shaping; (320.7110) Ultrafast nonlinear optics.

References and links

1. T. Brabec and F. Krausz, "Intense few-cycle laser fields: Frontiers of nonlinear optics," *Rev. Mod. Phys.* **72**, 545–591 (2000).
2. L. DiMauro and P. Agostini, "Ionization dynamics in strong laser fields," *Adv. At. Mol. Opt. Phys.* **35**, 79–120 (1995).
3. K. Burnett, V. C. Reed, and P. L. Knight, "Atoms in ultra-intense laser fields," *J. Phys. B At. Mol. Opt. Phys.* **26**, 561–598 (1993).
4. T. Brabec, *Strong Field Laser Physics* (Springer, 2009).
5. M. F. Kling, C. Siedschlag, A. J. Verhoef, J. I. Khan, M. Schultze, T. Uphues, Y. Ni, M. Uiberacker, M. Drescher, F. Krausz, and M. J. J. Vrakking, "Control of Electron Localization in Molecular Dissociation," *Science* **312**, 246–248 (2006).
6. A. Baltuška, T. Udem, M. Uiberacker, M. Hentschel, E. Goulielmakis, C. Gohle, R. Holzwarth, V. S. Yakovlev, A. Scrinzi, T. W. Hänsch, and F. Krausz, "Attosecond control of electronic processes by intense light fields," *Nature* **421**, 611–615 (2003).
7. M. R. Thompson, M. K. Thomas, P. F. Taday, J. H. Posthumus, A. J. Langley, L. J. Frasinski, and K. Codling, "One and two-colour studies of the dissociative ionization and Coulomb explosion of H₂ with intense Ti:sapphire laser pulses," *J. Phys. B At. Mol. Opt. Phys.* **30**, 5755–5772 (1997).
8. J. Wu, A. Vredenburg, L. P. H. Schmidt, T. Jahnke, A. Czasch, and R. Dörner, "Comparison of dissociative ionization of H₂, N₂, Ar₂, and CO by elliptically polarized two-color pulses," *Phys. Rev. A* **87**, 023406 (2013).
9. L. Zhang, X. Xie, S. Roither, Y. Zhou, P. Lu, D. Kartashov, M. Schöffler, D. Shafir, P. B. Corkum, A. Baltuška, A. Staudte, and M. Kitzler, "Subcycle Control of Electron-Electron Correlation in Double Ionization," *Phys. Rev. Lett.* **112**, 193002 (2014).
10. M. Shapiro, J. W. Hepburn, and P. Brumer, "Simplified laser control of unimolecular reactions: Simultaneous (ω_1 , ω_3) excitation," *Chem. Phys. Lett.* **149**, 451–454 (1988).
11. H. Li, X. Gong, K. Lin, R. de Vivie-Riedle, X. M. Tong, J. Wu, and M. F. Kling, "Sub-cycle directional control of the dissociative ionization of H₂ in tailored femtosecond laser fields," *J. Phys. B At. Mol. Opt. Phys.* **50**, 172001 (2017).
12. Q. Song, X. Gong, Q. Ji, K. Lin, H. Pan, J. Ding, H. Zeng, and J. Wu, "Directional deprotonation ionization of acetylene in asymmetric two-color laser fields," *J. Phys. B At. Mol. Opt. Phys.* **48**, 094007 (2015).
13. T. Endo, H. Fujise, Y. Kawachi, A. Ishihara, A. Matsuda, M. Fushitani, H. Kono, and A. Hishikawa, "Selective bond breaking of CO₂ in phase-locked two-color intense laser fields: laser field intensity dependence," *Phys. Chem. Chem. Phys.* **19**, 3550–3556 (2017).

14. D. W. Schumacher, F. Weihe, H. G. Muller, and P. H. Bucksbaum, "Phase Dependence of Intense Field Ionization: A Study Using Two Colors," *Phys. Rev. Lett.* **73**, 1344–1347 (1994).
15. H. G. Muller, P. H. Bucksbaum, D. W. Schumacher, and A. Zavriyev, "Above-threshold ionisation with a two-colour laser field," *J. Phys. B At. Mol. Opt. Phys.* **23**, 2761–2769 (1990).
16. D. Ray, F. He, W. Cao, H. Mashiko, P. Ranitovic, K. P. Singh, I. Znakovskaya, U. Thumm, G. G. Paulus, M. F. Kling, I. V. Litvinyuk, and C. L. Cocke, "Ion-Energy Dependence of Asymmetric Dissociation of D₂ by a Two-Color Laser Field," *Phys. Rev. Lett.* **103**, 223201 (2009).
17. B. Sheehy, B. Walker, and L. F. DiMauro, "Phase Control in the Two-Color Photodissociation of HD⁺," *Phys. Rev. Lett.* **74**, 4799–4802 (1995).
18. X. Xie, S. Roither, D. Kartashov, E. Persson, D. G. Arbó, L. Zhang, S. Gräfe, M. S. Schöffler, J. Burgdörfer, A. Baltuška, M. Kitzler, S. Gräfe, M. S. Schöffler, J. Burgdörfer, A. Baltuška, and M. Kitzler, "Attosecond Probe of Valence-Electron Wave Packets by Subcycle Sculpted Laser Fields," *Phys. Rev. Lett.* **108**, 193004 (2012).
19. Y. Mi, N. Camus, M. Laux, L. Fechner, R. Moshhammer, and T. Pfeifer, "Ionization of atoms and molecules in a strong two-color field," *J. Phys. Conf. Ser.* **635**, 092093 (2015).
20. Q. Song, P. Lu, X. Gong, Q. Ji, K. Lin, W. Zhang, J. Ma, H. Zeng, and J. Wu, "Dissociative double ionization of CO in orthogonal two-color laser fields," *Phys. Rev. A* **95**, 013406 (2017).
21. S. Eckart, M. Richter, M. Kunitski, A. Hartung, J. Rist, K. Henrichs, N. Schlott, H. Kang, T. Bauer, H. Sann, L. P. H. Schmidt, M. Schöffler, T. Jahnke, and R. Dörner, "Nonsequential Double Ionization by Counterrotating Circularly Polarized Two-Color Laser Fields," *Phys. Rev. Lett.* **117**, 133202 (2016).
22. S. De, I. Znakovskaya, D. Ray, F. Anis, N. G. Johnson, I. a. Bocharova, M. Magrakvelidze, B. D. Esry, C. L. Cocke, I. V. Litvinyuk, and M. F. Kling, "Field-Free Orientation of CO Molecules by Femtosecond Two-Color Laser Fields," *Phys. Rev. Lett.* **103**, 153002 (2009).
23. K. Oda, M. Hita, S. Minemoto, and H. Sakai, "All-optical molecular orientation," *Phys. Rev. Lett.* **104**, 1–4 (2010).
24. D. J. Cook and R. M. Hochstrasser, "Intense terahertz pulses by four-wave rectification in air," *Opt. Lett.* **25**, 1210 (2000).
25. P. Wei, J. Miao, Z. Zeng, C. Li, X. Ge, R. Li, and Z. Xu, "Selective Enhancement of a Single Harmonic Emission in a Driving Laser Field with Subcycle Waveform Control," *Phys. Rev. Lett.* **110**, 233903 (2013).
26. S. Haessler, T. Balčiūnas, G. Fan, L. E. Chipperfield, and A. Baltuška, "Enhanced multi-colour gating for the generation of high-power isolated attosecond pulses," *Sci. Rep.* **5**, 10084 (2015).
27. S. Watanabe, K. Kondo, Y. Nabekawa, A. Sagisaka, and Y. Kobayashi, "Two-Color Phase Control in Tunneling Ionization and Harmonic Generation by a Strong Laser Field and Its Third Harmonic," *Phys. Rev. Lett.* **73**, 2692–2896 (1994).
28. K. Kondo, Y. Kobayashi, A. Sagisaka, Y. Nabekawa, and S. Watanabe, "Tunneling ionization and harmonic generation in two-color fields," *J. Opt. Soc. Am. B* **13**, 424–429 (1996).
29. D. Xenakis, N. E. Karapanagioti, O. Faucher, E. Hertz, and D. Charalambidis, "Observation of field phase dependent autoionization," *J. Phys. B At. Mol. Opt. Phys.* **32**, 341–348 (1999).
30. C. Chen and D. S. Elliott, "Measurements of Optical Phase Variations Using Interfering Multiphoton Ionization Processes," *Phys. Rev. Lett.* **65**, 1737–1740 (1990).
31. M. Shapiro and P. Brumer, "Coherent control of molecular dynamics," *Reports Prog. Phys.* **66**, 859–942 (2003).
32. H. Xu, H. Hu, X.-M. Tong, P. Liu, R. Li, R. T. Sang, and I. V. Litvinyuk, "Coherent control of the dissociation probability of H₂ in ω - 3ω two-color fields," *Phys. Rev. A* **93**, 063416 (2016).
33. C. Jin, G. Wang, H. Wei, A.-T. Le, and C. D. Lin, "Waveforms for optimal sub-keV high-order harmonics with synthesized two- or three-colour laser fields," *Nat. Commun.* **5**, 4003 (2014).
34. L. Zhang, G.-L. Wang, and X.-X. Zhou, "Optimized two- and three-colour laser pulses for the intense terahertz wave generation," *J. Mod. Opt.* **63**, 2159–2165 (2016).
35. F. Krausz and M. Ivanov, "Attosecond physics," *Rev. Mod. Phys.* **81**, 163–234 (2009).
36. A. Wirth, M. T. Hassan, I. Grguras, J. Gagnon, A. Moulet, T. T. Luu, S. Pabst, R. Santra, Z. a. Alahmed, a. M. Azzeer, V. S. Yakovlev, V. Pervak, F. Krausz, and E. Goulielmakis, "Synthesized Light Transients," *Science* **334**, 195–200 (2011).
37. T. T. Luu, M. Garg, S. Y. Kruchinin, a. Moulet, M. T. Hassan, and E. Goulielmakis, "Extreme ultraviolet high-harmonic spectroscopy of solids," *Nature* **521**, 498–502 (2015).
38. M. Garg, M. Zhan, T. T. Luu, H. Lakhotia, T. Klostermann, A. Guggenmos, and E. Goulielmakis, "Multi-petahertz electronic metrology," *Nature* **538**, 359–363 (2016).
39. M. T. Hassan, T. T. Luu, A. Moulet, O. Raskazovskaya, P. Zhokhov, M. Garg, N. Karpowicz, a. M. Zheltikov, V. Pervak, F. Krausz, and E. Goulielmakis, "Optical attosecond pulses and tracking the nonlinear response of bound electrons," *Nature* **530**, 66–70 (2016).
40. H. Fattahi, H. G. Barros, M. Gorjan, S. Prinz, M. Haefner, M. Ueffing, A. Alismail, L. Vámos, A. Schwarz, O. Pronin, J. Brons, X. T. Geng, G. Arisholm, M. Ciappina, V. S. Yakovlev, D.-E. Kim, A. M. Azzeer, N. Karpowicz, D. Sutter, Z. Major, T. Metzger, and F. Krausz, "Third-generation femtosecond technology," *Optica* **1**, 45 (2014).
41. S.-W. Huang, G. Cirmi, J. Moses, K.-H. Hong, S. Bhardwaj, J. R. Birge, L.-J. Chen, E. Li, B. J. Eggleton, G. Cerullo, and F. X. Kärtner, "High-energy pulse synthesis with sub-cycle waveform control for strong-field physics," *Nat. Photonics* **5**, 475–479 (2011).
42. P. B. Corkum, "Plasma perspective on strong field multiphoton ionization," *Phys. Rev. Lett.* **71**, 1994–1997 (1993).

43. T. M. Kardaś, M. Nejbauer, P. Wnuk, B. Resan, C. Radzewicz, and P. Wasylczyk, "Full 3D modelling of pulse propagation enables efficient nonlinear frequency conversion with low energy laser pulses in a single-element tripler." *Sci. Rep.* **7**, 42889 (2017).
44. H. Ibrahim, B. Wales, S. Beaulieu, B. E. Schmidt, N. Thiré, E. P. Fowe, É. Bisson, C. T. Hebeisen, V. Wanie, M. Giguère, J.-C. Kieffer, M. Spanner, A. D. Bandrauk, J. Sanderson, M. S. Schuurman, and F. Légaré, "Tabletop imaging of structural evolutions in chemical reactions demonstrated for the acetylene cation," *Nat. Commun.* **5**, 4422 (2014).
45. J. Ullrich, R. Moshhammer, A. Dorn, R. Dörner, L. P. H. Schmidt, and H. Schmidt-Böcking, "Recoil-ion and electron momentum spectroscopy : reaction-microscopes," *Reports Prog. Phys.* **66**, 1463–1545 (2003).
46. T. Endo, H. Fujise, A. Matsuda, M. Fushitani, H. Kono, and A. Hishikawa, "Coincidence momentum imaging of asymmetric Coulomb explosion of CO₂ in phase-locked two-color intense laser fields," *J. Electron Spectros. Relat. Phenomena* **207**, 50–54 (2016).
47. V. Wanie, H. Ibrahim, S. Beaulieu, N. Thiré, B. E. Schmidt, Y. Deng, A. S. Alnaser, I. V. Litvinyuk, X.-M. Tong, and F. Légaré, "Coherent control of D₂ /H₂ dissociative ionization by a mid-infrared two-color laser field," *J. Phys. B At. Mol. Opt. Phys.* **49**, 025601 (2016).
48. X. M. Tong and C. D. Lin, "Empirical formula for static field ionization rates of atoms and molecules by lasers in the barrier-suppression regime," *J. Phys. B At. Mol. Opt. Phys.* **38**, 2593–2600 (2005).
49. M. V. Ammosov, N. B. Delone, and V. P. Krainov, "Tunnel Ionization Of Complex Atoms And Atomic Ions In Electromagnetic Field," *Sov. Phys. JETP* **64**, 138–141 (1986).
50. M. Kübel, C. Burger, N. G. Kling, T. Pischke, L. Beaufore, I. Ben-Itzhak, G. G. Paulus, J. Ullrich, T. Pfeifer, R. Moshhammer, M. F. Kling, and B. Bergues, "Complete characterization of single-cycle double ionization of argon from the nonsequential to the sequential ionization regime," *Phys. Rev. A* **93**, 053422 (2016).
51. M. G. Pullen, W. C. Wallace, D. E. Laban, A. J. Palmer, G. F. Hanne, A. N. Grum-Grzhimailo, K. Bartschat, I. Ivanov, A. Kheifets, D. Wells, H. M. Quiney, X. M. Tong, I. V. Litvinyuk, R. T. Sang, and D. Kiehlinski, "Measurement of laser intensities approaching 10¹⁵ W/cm² with an accuracy of 1%," *Phys. Rev. A* **87**, 053411 (2013).
52. C. A. Mancuso, K. M. Dorney, D. D. Hickstein, J. L. Chaloupka, X.-M. Tong, J. L. Ellis, H. C. Kapteyn, and M. M. Murnane, "Observation of ionization enhancement in two-color circularly polarized laser fields," *Phys. Rev. A* **96**, 023402 (2017).

1. Introduction

The interaction of atoms with ultrashort laser pulses has been studied for several decades [1–4]. Of recent interest is the interaction of matter with laser pulses of controlled waveform, such as few-cycle pulses with stable carrier-envelope phase or multi-cycle pulses composed of multiple colors. These waveform-controlled pulses permit a high degree of control of electron dynamics [5–7], and also over molecular processes [8–13].

Overlapping the fundamental and its second harmonic, in the following referred to as $\omega/2\omega$ fields, is a well-known method to control the ionization yield [14, 15] and steer the emission direction of electrons and ions [16, 17]. Such $\omega/2\omega$ fields based on pulses from Ti:sapphire lasers were employed to study electron dynamics in atoms [18, 19] and electron-nuclear dynamics in molecules [7, 16, 19]. In recent years these studies were extended to orthogonally polarized [20] or counter rotating $\omega/2\omega$ fields [21]. Furthermore, $\omega/2\omega$ fields can be used for all-optical orientation of molecules [22, 23], efficient terahertz generation [24], and increase the yield of high-harmonic generation (HHG) [25, 26].

Previous theoretical and experimental investigations using a composition of fundamental and third harmonic fields, in the following referred to as $\omega/3\omega$ fields, focused mainly on the yield in HHG, and the control of the ionization yield of atoms and molecules [10, 27–31]. As an example, Watanabe *et al.* [27] demonstrated that the yield in HHG can be increased by an order of magnitude upon addition of a 5 times less intense 3ω pulse to the fundamental laser pulse. In a recent publication Xu *et al.* presented the momentum distribution of protons after dissociation of H₂⁺ ions, where again a yield modulation in dependence of the relative phase was detected [32].

Theoretical reports show that a combination of all three laser fields will allow to further increase the HHG yield and eventually even support isolated attosecond bursts [33]. Moreover it was shown theoretically that such $\omega/2\omega/3\omega$ synthesized fields can be used to significantly enhance the generation of terahertz radiation [34]. The possibility of combining more than just two wavelengths opened the new field of sub-cycle pulse synthesis [35]. Since Wirth *et al.* [36]

demonstrated field synthesis of three independent channels obtained from dividing an 1.5-octaves white light generated in a hollow core fiber, the coherent addition of spectrally separated beams became an important tool in strong field physics [37, 38]. Such sub-cycle waveforms opened the possibility of generating optical pulses with sub-femtosecond duration, which was successfully used for probing attosecond electron dynamics [39]. Another approach relies on the coherent combination of pulses from optical parametric amplifiers operating at different wavelengths [40]. This approach was demonstrated in the mid-infrared region with microjoule pulse energies [41]. Due to the relatively long optical beam paths, however, such a device requires active stabilization of the interferometer with attosecond precision. From the experimental point of view, both approaches represent a significant challenge making simpler designs of field synthesis desirable. Utilizing three color $\omega/2\omega/3\omega$ fields, generated from a Ti:sapphire laser, was demonstrated by Wei *et al.* [25], where selective enhancement of a single high harmonic in argon gas was achieved. Although the approach seems to be very simple and stable, it inherently did not permit an independent control of the delay between the three colors. Moreover, the polarizations of the beams were fixed (the polarization of the second harmonic beam was perpendicular to the other beams), thus significantly limiting its applicability. To overcome those limitations, here we introduce a device, which combines the advantage of both approaches: the simplicity of optical nonlinear harmonic conversion with the flexibility of field synthesis.

In the following we demonstrate the efficient generation of the second and third harmonic of a femtosecond laser pulse from a Ti:sapphire laser system, followed by a compact and versatile three-color synthesizer. The output of the synthesizer is used to investigate the interaction of neon with the combined $\omega/2\omega$ and $\omega/3\omega$ laser fields by measuring the momentum distribution of Ne^+ ions from the strong-field ionization of neon. To interpret new experimental findings, we compare the measured data with semi-classical simulations based on the simple man's model [42].

2. Multi-color-pulse generation and synthesis

The setup for generating the second and third harmonic of the driving field and for three-color synthesis is schematically shown in Fig. 1. The setup is based on a Ti:sapphire laser system with pulse durations down to 25 fs and an energy of up to $720 \mu\text{J}$ at a repetition rate of 10 kHz (Femtopower Compact Pro HR, Spectra Physics). We took special care to achieve a high yield

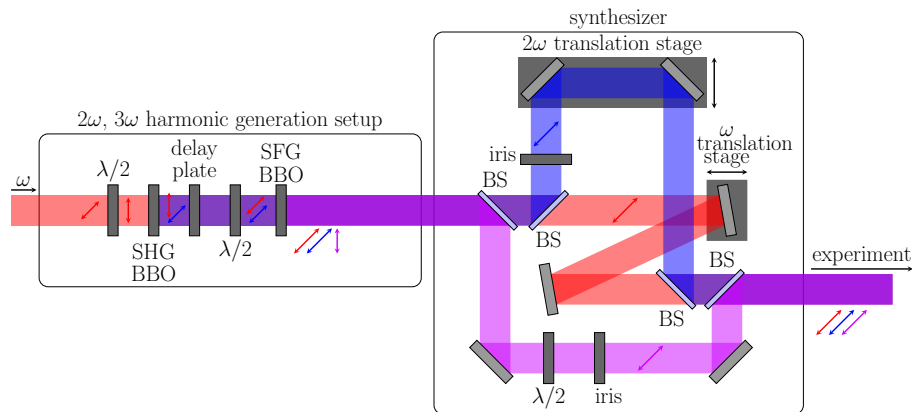


Fig. 1. Experimental setup for the multi-color pulse generation and synthesis. SHG: second harmonic generation, SFG: sum frequency generation, BBO: β -barium-borate crystal, BS: beamsplitter, $\lambda/2$: half waveplate.

in sum frequency generation (SFG), which was done in a collinear configuration, following the

idea proposed by Kardaś *et al.* [43], and the experimental implementation by Ibrahim *et al.* [44] In short, the laser passes through the following series of optical components: a 200 μm thick β -barium borate (BBO) crystal cut at 27.2° for second harmonic generation (SHG), a birefringent material to retard the fundamental beam (450 μm thick BBO cut at 70°), a $\lambda/2$ quartz wave-plate to rotate the fundamental beam with respect to the second harmonic, and a 100 μm thick BBO cut at 44.3° , where sum frequency mixing allows for efficient SFG. In the second part of the setup, the second and third harmonic beams are separated from the fundamental beam using a combination of a custom-made triple band dichroic beamsplitters (BS) facilitating low group delay dispersion (below 50 fs^2), and supporting the full bandwidth of each harmonic. Each coating supports high reflectivity (above 99%) at 45° and high transmission (above 99%) for each corresponding harmonic. The beamsplitters were fabricated on 1 mm thick substrates made of fused silica to minimize additional pulse elongation. An anti-reflection coating, of similar thickness as the front coating, was applied on the back side of the BS for two reasons: First, to prevent a post pulse created from the Fresnel reflection on the back side of the optic. Secondly, to reduce stress induced by the single side coating of the thin substrate, which would result in avoidable wavefront distortions. Such separation of the harmonics into individual channels enables that each color could be independently controlled with respect to energy, delay and its polarization. The colors corresponded to central wavelengths of 790 nm (ω), 395 nm (2ω), and 263 nm (3ω), see Fig. 2. The electric field composed of all three colors can be written as:

$$E(t, \phi_2, \phi_3) = E_\omega \cos(\omega t) + E_{2\omega} \cos(2\omega t + \phi_2) + E_{3\omega} \cos(3\omega t + \phi_3), \quad (1)$$

where $E_{\omega,2\omega,3\omega}$ represent the amplitudes of the electric field, ω is the fundamental frequency, and $\phi_{2,3}$ denote the relative phase between the fundamental and the second or third harmonic, respectively. This relative phase, which can be translated into the relative delay between the synthesizer arms, is controlled by nanometer-precision delay stages. To achieve high passive stability of the synthesizer, optical mounts were carefully chosen to avoid mechanical resonances, verified by recording the interference stability using a reference continuous wave (cw) laser. Additionally, the setup was housed to avoid air fluctuations. Thanks to the compact footprint of the synthesizer (each beam path is around 30 cm), and isolation from environmental disturbances, passive sub-100-mrad stability over a 15-min timescale was achieved. In order to account for unavoidable long term drifts we continuously swept the delay stage between 0 and 4π (one complete sweep within 10 minutes). These short term measurements were then analyzed individually. Any phase drifts between these short term measurements were shifted to the starting value within the post analysis enabling a combination of all measurements for the complete measuring time of 12 hours. Within these 12 hours a slow total phase drift of $\pi/2$ was observed, which had to be compensated by the post analysis.

An efficient frequency conversion of short pulses becomes a challenging task. It is often a compromise between conversion efficiency (requiring longer crystals and higher intensities) and pulse duration, which is elongated by the group velocity mismatch between interacting beams in the conversion crystals. Careful numerical simulation of the third harmonic generation using a nonlinear propagation software [43] provided optimal parameters for the intensities, and crystals thickness, which allowed for obtaining high conversions efficiency, while only slightly elongating the pulses in time. With an input energy of 650 μJ in front of the frequency converter and an intensity of 160 GW/cm^2 , we were able to generate the three colors with respective final energies of 350 μJ (ω), 90 μJ (2ω), and 80 μJ (3ω) at the output of the synthesizer. This corresponds to over 12 % conversion into the third harmonic, including losses in the synthesizer setup. According to the simulations, after the harmonic generation setup all beams have close to Gaussian beam profiles. It was further verified by recording in the focal plane Gaussian distributions for each harmonic. In Fig. 2(a) the calculated evolution of energies of all three harmonics during nonlinear propagation inside second BBO crystal is shown. Discrepancies between calculated and measured

pulse energies are due to an uncertainty of the crystals thickness (which is typically tens of micrometers for such thin crystals). Moreover, the simulation does not include optical losses on the optical interfaces in the harmonic generation setup as well as the waveform synthesizer. Measured spectra of the three beams after the field synthesizer are shown in Fig. 2(b) as red lines and correspond well to the calculated ones, shown as black lines.

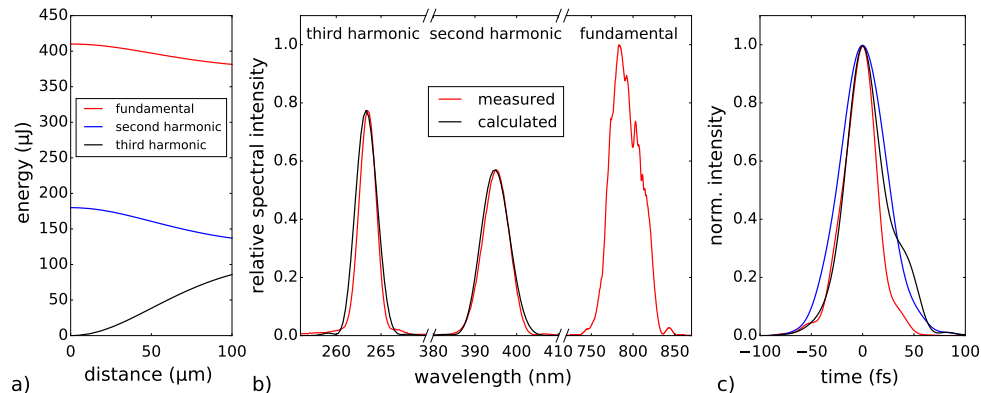


Fig. 2. (a) Simulated evolution of pulse energies of all three harmonics of the sum-frequency mixing process within the second BBO-crystal. (b) Measured (red) and calculated (black) spectra of the fundamental, second harmonic and third harmonic. While the height of the fundamental beam is normalized, the spectral intensities of the second and third harmonic are calculated according to their relative pulse energies. (c) Calculated temporal profiles of the three beams after propagation through dispersive media.

Due to the propagation through dispersive material in the field synthesizer, additional 2 m of air, and the entrance window (1 mm SiO_2) into the experimental chamber, the pulses get stretched in time. The resulting calculated temporal profiles for the three beams in the interaction region are shown in Fig. 2(c) with temporal full-width-at-half-maxima (FWHM) of 35 fs, 52 fs, and 41 fs for the fundamental, second and third harmonic, respectively. The pulse duration of the fundamental pulse was verified by TG-FROG measurements, while cross-correlation measurements were used for the second and third harmonic. The retrieved pulse durations are 35 fs (ω), 61 fs (2ω), and 59 fs (3ω), cf. Table 1. The discrepancies could be the result of higher nonlinearities experienced by the second and third harmonic during propagation through the dispersive elements. To decrease the pulse duration down to the Fourier limit one could introduce chirped mirrors in each arm of the synthesizer at the cost of a longer beam path making the synthesizer more complex, and reducing the throughput.

For the experiments on neon, the polarization of the 3ω beam is turned by 90 degrees to achieve parallel polarization of all three colors. Additionally, the size of the third harmonic beam was adjusted via an iris to match the focal spot size of the fundamental beam. Afterwards, the beams are recombined and sent directly into the experimental chamber. The experimental setup consists of a reaction microscope (REMI), which allows retrieving the 3D momentum of each ionized particle on a single shot basis. More details about the REMI can be found in the review by Ullrich *et al.* [45]. The spectrum, the pulse energy and the focal spot size were determined before and after each measurement in front of the REMI. A summary of the laser parameters is shown in Table 1. It is worth mentioning that only a small fraction of the pulse energies were needed for the presented experiments. The intensities were chosen such that the observable shifts in momentum distribution became as clear as possible while background signal from ionization by a single harmonic was minimized. We estimate that the numbers in Tab. 1 for the intensities, pulse durations, and focus sizes have an uncertainty of about 20 %, which, however, is not crucial

for the observed control.

Table 1. The laser parameters of the fundamental, second harmonic and third harmonic for the measurements using $\omega/2\omega$ and $\omega/3\omega$ configurations. The two applied energies of the fundamental beam for the two sets of measurements are shown along with the corresponding intensities.

	Wavelength (nm)	Pulse energy (μJ)	τ_{FWHM} (fs)	Focus size (μm)	Intensity (10^{13} W/cm^2)
ω (in $\omega/2\omega$ fields)	790	39	35	40	6.1
ω (in $\omega/3\omega$ fields)	790	76	35	40	12
2ω	395	27	61	31	4.1
3ω	263	10	59	35	1.3

3. Results and discussion

To proof the applicability of the synthesizer we measured the momentum distribution of Ne^+ in $\omega/2\omega$ fields. In Fig. 3, we present the dependence of ionization yield of neon on the ion momentum and relative two-color phase ϕ_2 . The observed horizontal stripes correspond to peaks from above-threshold ionization (ATI) and are in good agreement with peak positions calculated from the photon energy of the fundamental light (shown in grey in the left panel). In agreement with earlier work, we observe the final momentum with characteristic oscillations as a function of the relative phase [18, 19].

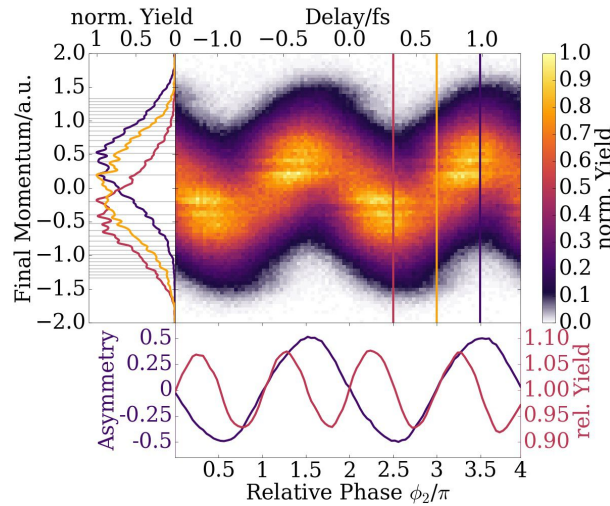


Fig. 3. Control over neon ionization in $\omega/2\omega$ fields. The ionization yield is plotted as a function of momentum along the polarization direction and relative phase of the two-color ($\omega/2\omega$) field. The lower panel presents the relative total yield, abbreviated as 'rel. Yield' (red), and the asymmetry of ion emission direction (purple). In the left panel the momentum distributions at the three indicated relative phases are plotted.

In order to quantify the phase-dependent momentum shifts, we define an asymmetry parameter $A(\phi)$ as:

$$A(\phi) = \frac{L(\phi) - R(\phi)}{L(\phi) + R(\phi)}, \quad (2)$$

where $L(\phi)$ and $R(\phi)$ denote the yield of ions emitted with positive and negative momentum along the laser polarization direction, respectively. The resulting asymmetry $A(\phi)$ is plotted in the lower panel together with the relative total ion yield, where unity corresponds to the phase averaged mean yield. The π -periodicity of the total yield results from occurrences of field crests resulting in enhanced ionization twice per fundamental laser period. The asymmetry oscillates with a periodicity of 2π and its amplitude (50 %) demonstrates excellent control over the ion emission direction. This experiment clearly shows that strong control over the direction of electron emission can be achieved with such synthesized waveforms. This will allow e.g. to steer various molecular processes, compare Refs. [13, 16, 46, 47].

In the following, we present experimental and theoretical results on the control of the ionization of neon in $\omega/3\omega$ fields. In Fig. 4, we show the ionization yield as a function of the momentum and

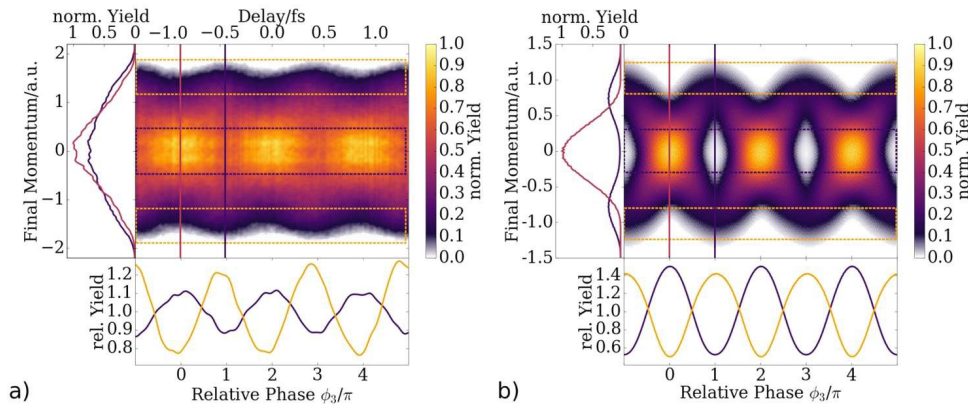


Fig. 4. Control of neon ionization in $\omega/3\omega$ fields. The ionization yield is presented in dependence of the Ne^+ momentum along the polarization direction and the relative phase between the laser fields for (a) experimental and (b) calculated results. In the lower panels the integrated ionization yield is shown for the areas marked by correspondingly colored dashed lines while the left panel presents the momentum distribution along the line cuts in the 2D plot.

the relative phase between the ω and 3ω fields for experimental (a) and theoretical (b) results. The relative phase was varied from 0 to 6π to confirm the periodicity of the observed pattern. Similar to the $\omega/2\omega$ case, we again observe ATI peaks originating from the fundamental wavelength. More dominant, however, is the broadening of the momentum distribution for phases that are odd multiples of π . This broadening is highlighted by two selected momentum spectra, see Fig. 4(a), for positions depicted by the two vertical lines in the experimental results.

In order to understand the underlying physics behind the observed control of Ne^+ momenta in $\omega/3\omega$ fields, we have used semi-classical simulations based on the simple man's model [42], in which the ionization rate is calculated by the formula of Ref. [48] – a modification of the initial formula from Ammosov, Delone, and Krainov (ADK) for ionization in a quasi-static field [49]. This modification allows covering the tunnel ionization regime as well as the barrier suppression regime [48]. After ionization, the electron is propagated classically along the polarization direction neglecting all interactions with the parent ion. The two-color field is described as:

$$E = E_\omega \cos(\omega t) + E_{3\omega} \cos(3\omega t + \phi_3), \quad (3)$$

where ϕ_3 denotes the relative phase between the fundamental and the third harmonic. In the simulations, the intensity averaging over the focal volume is taken into account assuming a Gaussian intensity profile and neglecting intensity variation along the beam propagation axis.

The latter assumption is reasonable since the Rayleigh-lengths for all colors was more than 4 mm, exceeding the dimension of the gas jet (several 100 μm) in the REMI. We find best agreement with the momentum shifts observed in the experiments when the intensities used in the simulation are 3 times higher than the experimentally retrieved intensities. The fact that electron momenta are systematically underestimated in a semi-classical approach is known (see for instance [50,51]). We note that the simple model cannot capture all details of the process, however we like to emphasize that a higher-level of theory was not essential here, since the results rather serve to demonstrate the capabilities of the waveform synthesizer.

When we compare our experimental results to the simulations, we find qualitative agreement with respect to the observed phase control of the ionization yield and the shift in the oscillatory patterns at low and high Ne^+ momenta. To investigate the yield modulations in more detail, we separate two momentum regions: high momenta, marked by yellow rectangles, and low momenta, depicted in purple. The corresponding integrated signals are shown in the lower graph. The phase dependent modulation of the yield for low momenta amounts to 10 %, while the modulation depth increases to 20 % for high momenta. A phase-independent signal at low momenta is seen in the experimental data, which likely contributes to the smaller modulation at low momenta. Intensity fluctuations are unlikely to cause this background, since simulations show that the momentum shifts should still be observed for intensities varied by one order of magnitude. We believe that the constant background can rather be attributed to situations, where an atom only experiences one laser field and therefore is not sensitive to the combined fields, i.e. an imperfect overlap of the two fields in the focus. Moreover, a phase shift of π is observed between the low and high momentum region, which is also retrieved in the simulations.

In order to better understand the atom-laser interaction in the case of $\omega/3\omega$ fields, we present in Fig. 5 the calculated electric field (solid purple line), the corresponding final momentum (dashed green line), the ionization rate calculated by the ADK rate (grey area), and the final momentum distribution (green area on the right) for two different relative phases ϕ_3 .

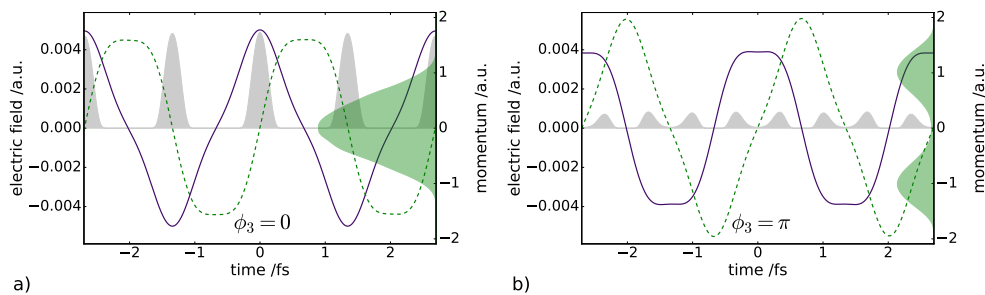


Fig. 5. Control of Ne ionization yield and Ne^+ momenta in $\omega/3\omega$ fields. Depicted are the electrical field (solid purple line), the ionization rate (grey area) and the final momentum (dashed green line) and its distribution (green area) for relative phases of $\phi_3 = 0$ in a), $\phi_3 = \pi$ in b), respectively.

For a relative phase of zero, we see that the final momentum distribution is centred around zero as it would be expected from ionization in just a single-color field. Increasing the relative phase to π , we observe two phenomena: First, the overall ionization rate becomes lower, which was previously seen in several calculations and measurements [28,29]. This decreased ionization yield results from lower absolute fields and hence lower ionization rates. Secondly, a splitting of the final momentum distribution becomes clearly visible. This splitting can be related to the vector potential. For a relative phase of π , the ionization rate is highest for times when the final

momentum is non-zero. Depending on the cycle of the ionization, the final momentum is either negative or positive. Furthermore, the range of the final momenta increased by 50 % compared to a relative phase of zero. It is also important to notice that the ionization yield for a relative phase of π is 8 times lower than for a relative phase of zero. Therefore, in an experiment, which is only sensitive to the overall ionization yield, a 2π -periodic modulation would be observed, with lowest yield corresponding to a phase of π [27, 29, 30].

While many recent studies use orthogonally polarized [20] or counter-rotating circular polarized $\omega/2\omega$ fields [21, 52], the three-color device introduced here permits tailoring the fields with all three colors and thereby extend such studies to more complex fields. Using such tailored laser fields is also expected to be very beneficial for high-harmonic generation [33]. Another application of the three-color setup are pump-probe experiments, where e.g. the ultraviolet pulse is used for exciting the target and the $\omega/2\omega$ laser field is used for coherent control. This is particularly interesting in studies on the strong-field control of molecular reactions. As an example, acetylene, a commonly investigated molecule in strong-field physics, can be excited by the third harmonic (as was done in e.g. [44]) and the isomerization to vinylidene can be controlled with the $\omega/2\omega$ field near conical intersections.

4. Conclusion

In conclusion, we presented a device for the efficient generation of the second and third harmonic of a femtosecond laser field in a collinear geometry, while preserving short pulse durations. A subsequent multi-harmonic synthesizer permits to superimpose all three colors and control their relative phase as well as their intensities and polarizations. We used the device in experimental work on the interaction of $\omega/2\omega$ and $\omega/3\omega$ fields with neon atoms. For $\omega/3\omega$ fields, we observed a modulation of the ionization yield and ion momenta as a function of the relative phase between both colors. A shift of π is observed between the phase-dependent oscillations of low and high ion momenta. These trends were retrieved by semi-classical simulations based on the simple man's model. The three-color device offers sufficient flexibility for a variety of future studies on the coherent control of strong-field processes and for time-resolving ultrafast molecular dynamics.

Funding

Max Planck Society and by the German Research Foundation via LMUexcellent and via the Cluster of Excellence: Munich Centre for Advanced Photonics (MAP). Mobility Plus fellowship from the Polish Ministry of Science and Higher Education (no. 1283/MOB/IV/2015/0).